[Supporting Information to accompany]

Imine-Linked Microporous Polymer Organic Frameworks

Prativa Pandey, Alexandros P. Katsoulidis, Ibrahim Eryazici, Yuyang Wu, Mercouri G. Kanatzidis, SonBinh.T.Nguyen**

Department of Chemistry, Northwestern University, 2145 Sheridan Road, Evanston, Illinois 60208-3113, USA.
*Email: m-kanatzidis@northwestern.edu, stn@northwestern.edu.

Table of Content

S1. Synthesis of 1,3,5-triformylbenzene (A1).

Scheme S1. Synthesis of 1,3,5-triformylbenzene (**A1**).

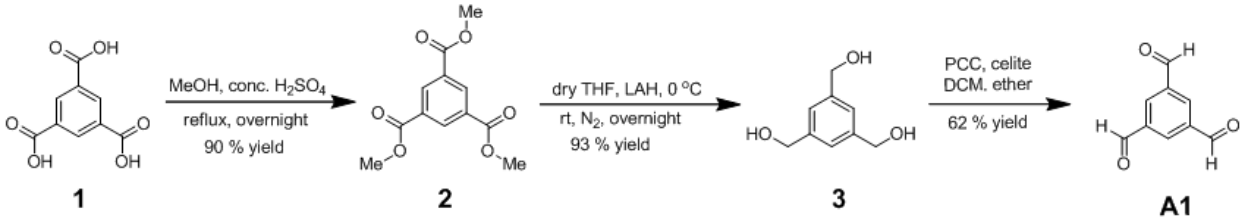

^{1}H NMR data are reported as follows: chemical shift (multiplicity (b = broad singlet, s = singlet, d = doublet,), integration, and peak assignments, coupling constants). ^{1}H and ^{13}C chemical shifts are reported in ppm from TMS with the residual solvent resonances as internal standards. $CDCl_3$ was used an NMR solvent.

Synthesis of trimethyl-1,3,5-benzenetricarboxylate (2). Compound **2** was synthesized following a previously reported procedure.[S1] Typical yield for a 38-mmol (8 g) reaction is 34.5 mmol (7.7 g, 90%). ^{1}H NMR: δ 3.9 (s, 9H, OC*H*$_3$), 8.8 (s, 3H, aromatic-*H*). ^{13}C NMR : δ 51.5 (O*C*H$_3$), 134.5 (Ar$_{2,4,6}$-*C*), 137.0 (Ar$_{2,4,6}$-*C*), 165.8 (*C*O$_2$CH$_3$).

Synthesis of 1,3,5-tris(hydroxymethyl)benzene (3). This synthesis was conducted under nitrogen following a previously reported procedures.[S2] The reaction time was increased from 4 h to 10 h to obtain higher yield (reported yield = 73 %, obtained yield = 93% for a 38-mmol (8 g) reaction). ^{1}H NMR: δ 4.50 (s, 6H, C*H*$_2$OH), 5.1 (bs, 3H, CH$_2$O*H*), 7.18 (s, 3H, Ar$_{2,4,6}$-*H*). ^{13}C NMR : δ 62.96 (*C*H$_2$OH), 122.89 (Ar$_{2,4,6}$-*C*), 142.02 (Ar$_{1,3,5}$-*C*).

Synthesis of 1,3,5-triformylbenzene (A1). This synthesis is a modification of a previously reported procedures.[S2] To a stirring mixture of pyridinium chlorochromate (PCC, 5.28 g, 24.5 mmol) and Celite (4 g) in CH_2Cl_2 (120 mL), was added solid 1,3,5-tris(hydroxymethyl)benzene (**3**, 0.99 g, 5.9 mmol). After 10 h, the reaction mixture was diluted with ether (20 mL) and was allowed to stir for 30 min. The reaction mixture was then filtered through a bed of Celite and the Celite bed was further washed with CH_2Cl_2 (100 mL). The combined filtrate was concentrated to dryness on a rotary evaporator and the obtained crude product purified by flash chromatography (100 % CH_2Cl_2) to afford **4** as white solid (602 mg, 62% yield). ^{1}H NMR : δ 8.66 (s, 3H, Ar$_{2,4,6}$-*H*), 10.21 (s, 3H, C*H*O). ^{13}C NMR : δ 135.6 (Ar$_{2,4,6}$-*C*), 137.9 (Ar$_{1,3,5}$-*C*), 191.0 (*C*HO). FTIR (KBr pellet): See Figure S13.

S2. Effect of temperature, monomer concentration, and solvent on the pore properties of polymer A1-B2.

Table S1. Effect of temperature, monomer concentration, and solvent on the pore properties of POF **A1**-**B2**.

Entry	Temperature profile	Solvent	Amine functional group concentration	Specific surface area ($m^2 g^{-1}$)	Micropore volume ($cm^3 g^{-1}$)	Total pore volume ($cm^3 g^{-1}$)	Yield (%)
1	180 ˚C, 24 h	Mesitylene	0.48	0	n.a.[a]	n.a.[a]	41
2	180 ˚C, 24 h	Dioxane	0.48	80	n.a.[a]	n.a.[a]	58
3	180 ˚C, 24 h	NMP	0.48	568	0.19	0.67	62
4	180 ˚C, 24 h	DMF	0.48	921	0.33	0.88	97
5	180 ˚C, 12 h	DMSO	0.48	865	0.29	0.87	65
6 (Table 1, entry 2a)	180 ˚C, 24 h	DMSO	0.48	1063	0.31	1.13	98
7 (Table 1, entry 2c)	125 ˚C, 24h	DMSO	0.48	583	0.19	0.43	71
8	125 ˚C, 3h 180 ˚C, 24h	DMSO	0.48	532	0.17	0.45	64
9	160 ˚C, 24h	DMSO	0.48	1035	0.32	1.10	96
10	170˚C, 24h	DMSO	0.48	1023	0.31	0.99	95
11	190 ˚C, 24h	DMSO	0.48	1045	0.36	0.99	98
12	180 ˚C, 24 h	DMSO	0.34	656	0.21	0.57	69
13	180 ˚C, 24 h	DMSO	0.40	807	0.23	0.76	76
14 (Table 1, entry 2a)	180 ˚C, 24 h	DMSO	0.48	1063	0.31	1.13	98
15	180 ˚C, 24 h	DMSO	0.60	823	0.28	0.78	85
16	180 ˚C, 24 h	DMSO	0.80	659	0.22	0.63	70

[a] The solids obtained have negligible N_2-uptake

S3. FTIR, GC, ^{13}C CPMAS NMR, and N_2 adsorption-desorption data for end-capping experiments.

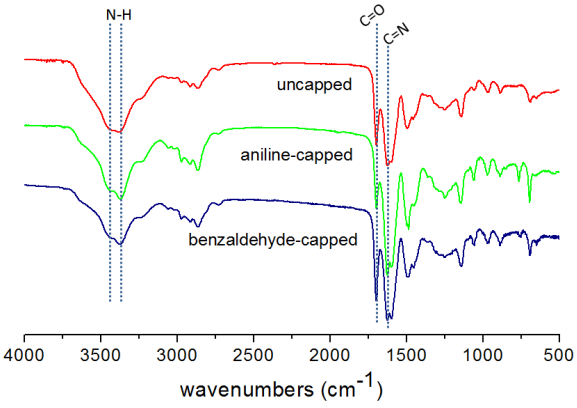

Figure S1. FTIR spectra of uncapped POF **A1**-**B2** (Table S2, entry 1), aniline-capped POF **A1**-**B2** (Table S2, entry 2), and benzaldehyde-capped POF **A1**-**B2** (Table S2, entry 3).

Table S2. Pore properties analysis of the end-capped POF **A1-B2**.

Entry	POF **A1-B2** (Table S1, entry 11)	Specific surface area ($m^2 g^{-1}$)	Micropore volume ($cm^3 g^{-1}$)	Total pore volume ($cm^3 g^{-1}$)
1	uncapped	1045	0.36	0.99
2	aniline-capped	1057	0.39	1.05
3	benzaldehyde-capped	1079	0.34	1.07

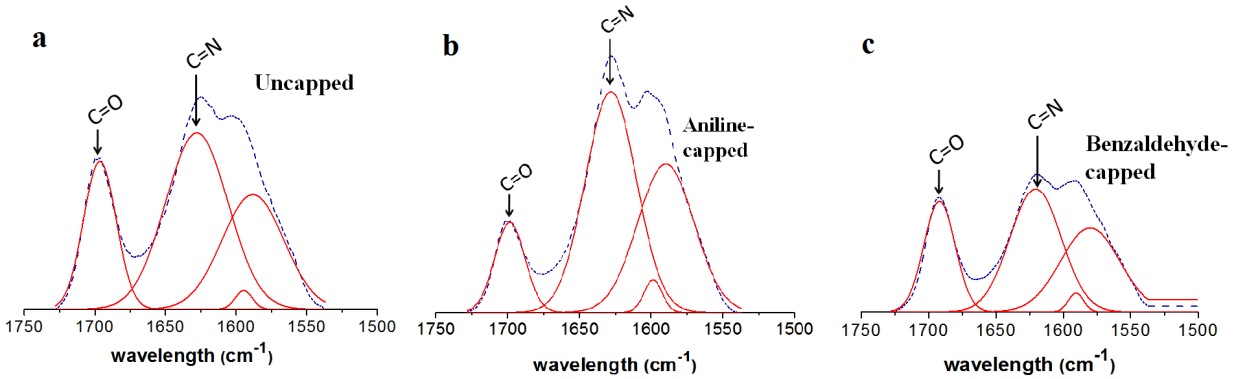

Figure S2. **a**. FTIR spectrum of uncapped POF **A1-B2** (Table S2, entry 1) peak-fitted in the region 1730-1525 cm^{-1}. **b**. FTIR spectrum of aniline-capped POF **A1-B2** (Table S2, entry 2) peak-fitted in the region 1730-1525 cm^{-1}. **c**. FTIR spectrum of benzaldehyde-capped POF **A1-B2** (Table S2, entry 3) peak-fitted in the region 1730-1525 cm^{-1}.

Assuming that the imine and carbonyl stretches have similar IR absorption cross-sections, by comparing the integrated carbonyl and imine peak areas in the IR spectra of uncapped and aniline-capped POFs **A1-B2** (cf. Tables S3 and S4, respectively), it appears that there are unreacted carbonyl groups in the uncapped POFs. This carbonyl peak decreases from ~30% to ~20% of the total [imine + carabonyl] peak area after the aniline-capping experiment, indicating that about 1/3 of the unreacted carbonyl groups have been capped and the remaining 2/3 might not be accessible to the capping agents.

Estimates of the amount of unreacted amine groups in the as-synthesized (uncapped) POF cannot be extracted from the benzaldehyde-capped experiment. After the benzaldehyde capping experiment, we observed a significant increase in the relative ratio of carbonyl/imine peak compared to that in the uncapped POF (Figure S2). We atrributed this to the physisorption of benzaldehyde capping agent in the pores of POF **A1-B2**; however, it is possible that the added benzaldehyde also caused trans-imination to occur, releasing some of the formyl group in the **A1** unit of the POF.

Table S3. Tabulation of integrated carbonyl (C=O) and imine (C=N) peak areas in uncapped POF **A1-B2** (Table S2, entry 1) after peak fitting.

Stretch	Wavelength (cm^{-1})	Normalized Area	Relative Area
C=O	1700	780.80	30.5%
C=N	1625	1779.91	69.5%

Table S4. Tabulation of integrated carbonyl (C=O) and imine (C=N) peak areas in aniline-capped POF **A1**-**B2** (Table S2, entry 2) after peak fitting.

Stretch	Wavelength (cm^{-1})	Normalized Area	Relative Area
C=O	1700	437.66	19.5%
C=N	1625	1808.58	80.5%

Table S5. Tabulation of integrated carbonyl (C=O) and imine (C=N) peak areas in benzaldehyde-capped POF **A1**-**B2** (Table S2, entry 3) after peak fitting.

Stretch	Wavelength (cm^{-1})	Normalized Area	Relative Area
C=O	1700	418.72	35.5%
C=N	1625	761.77	64.5%

Assuming the starting materials had fully reacted during the synthesis of POF **A1**-**B2** (Table S1, entry 11) and the amount of water eliminated is negligible, we calculated that the 350 mg of POF used in each end-capping experiment had ~3 mmol of imine (C=N) functional groups. As observed from GC analysis data, 0.66 mmol out of the 3.2 mmol aniline capping agent was consumed in the first end-capping experiment (Table S6, 20.6% aniline consumed). Similarly, 0.51 mmol out of the 3.2 mmol benzaldehyde capping agent was consumed in the second end-capping experiment (Table S7, 21% benzaldehyde consumed). Overall, the GC analysis suggested that ~22% of amine or aldehyde groups present in the POF remained unreacted during the synthesis. However, due to the possibilities that some of these unreacted group will not be accessible to the capping agent and that some of the capping agent can physisorb in the pores of the POF (see FTIR analysis above), this value is only a rough estimate.

Table S6. GC analysis of the mother liquor in aniline end-capping experiment.

Time (h)	Mesilytene peak area	Aniline peak area	[Aniline/Mesitylene] Ratio	Amount of remaining aniline (mmol)	Amount of aniline consumed (mmol)	Estimated amount of unreacted aldehyde present in POF(%)
0.25	505700	222447	0.44	3.08	0.12	4.03
0.5	416501	179058	0.43	3.02	0.18	6.04
1	355444	148669	0.42	2.96	0.24	8.05
3	394828	158451	0.40	2.84	0.36	12.08
5	412365	159244	0.39	2.78	0.42	14.09
9	428914	162316	0.38	2.72	0.48	16.10
16	502703	188562	0.37	2.66	0.54	18.11
18	475946	166888	0.35	2.54	0.66	22.14
20	637896	223143	0.35	2.54	0.66	22.14

Table S7. GC analysis of the mother liquor in benzaldehyde end-capping experiment.

Time (h)	Mesilytene peak area	Benzaldehyde peak area	[Benzaldehyde/Mesitylene] ratio	Amount of remaining benzaldehyde (mmol)	Amount of benzaldehyde consumed (mmol)	Estimated amount of unreacted aniline present in POF (%)
0.25	337804	169033	0.50	3.09	0.11	3.74
0.5	405460	195946	0.48	2.98	0.22	7.49
1	366867	174165	0.47	2.92	0.28	9.36
3	377487	174005	0.46	2.86	0.34	11.23
5	386703	178674	0.46	2.86	0.34	11.23
9	465318	208554	0.45	2.81	0.39	13.10
16	358756	153731	0.43	2.69	0.51	16.84
18	387592	158334	0.41	2.58	0.62	20.58
20	264246	104803	0.40	2.53	0.67	22.46

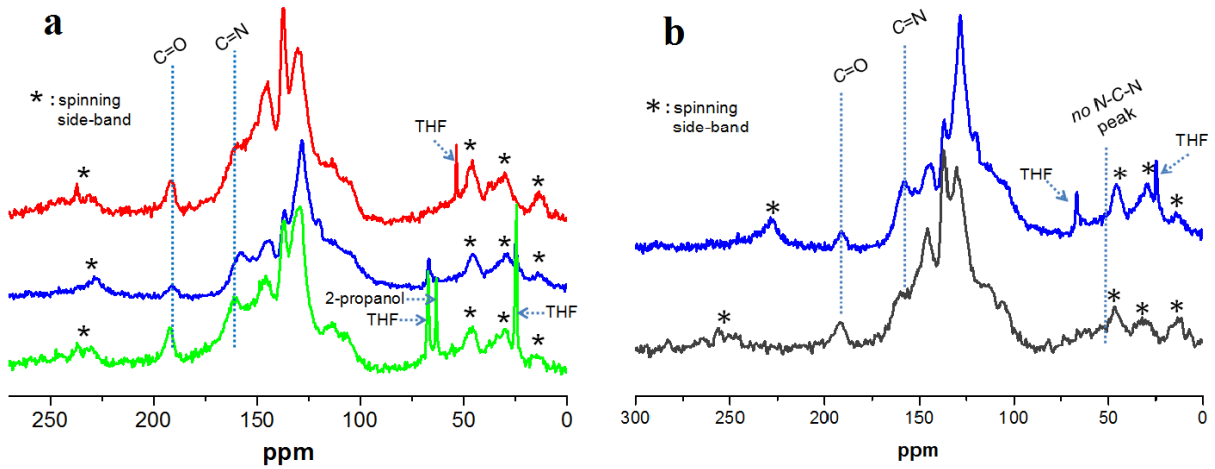

Figure S3. (a) ^{13}C CPMAS (10k Hz) NMR spectra of as-synthesized uncapped POF **A1**-**B2** (Table S2, entry 1), aniline-capped POF **A1**-**B2** (Table S2, entry 2), and benzaldehyde-capped POF **A1**-**B2** (Table S2, entry 3). The THF signals are quite strong in the capped samples because THF was used as the solvent in the capping reaction. (b) ^{13}C CPMAS NMR (spinning rate: 10k Hz (top) and 12k Hz (bottom)) spectra of vacuum-dried aniline-capped POF **A1**-**B2** (Table S2, entry 2) showing the absence of aminal (N-C-N) peak. The size of the spinning side-bands below 50 ppm is greatly reduced in the 12k Hz spectra.

While the formation of aminal, as reported by the Müllen group,[S3] is a potential product in our aniline-capped experiment, we note that the melamine used by these researchers is very different from the aniline in our experiments and their respective condensations with benzaldehyde cannot be compared. As shown in Müllen's report, imine of melamine are well-known to undergo secondary Michael reaction with a second equivalent of amino group to yield aminal while aniline does not. Other aromatic azines behave similarly. For example, 2-aminopyridine, a "partial-triazine" analog of the melamine ring will form stable aminal with benzaldehyde.[S4-S5] When the aniline is 3-aminopyridine, a non-azine aniline, only the Schiff base is formed in the reaction with benzaldehyde.[S6] Indeed, aniline-based aminal are only stable for straight-chain aliphatic aldehydes.[S7-S8]

Given the aforementioned precedents, we are confident that our aniline-capped experiments did not result in aminals. In addition, the ^{13}C CPMAS NMR spectrum of the POFs (Figure S3b) does not show any resonance that can be attributed to an aminal moiety.

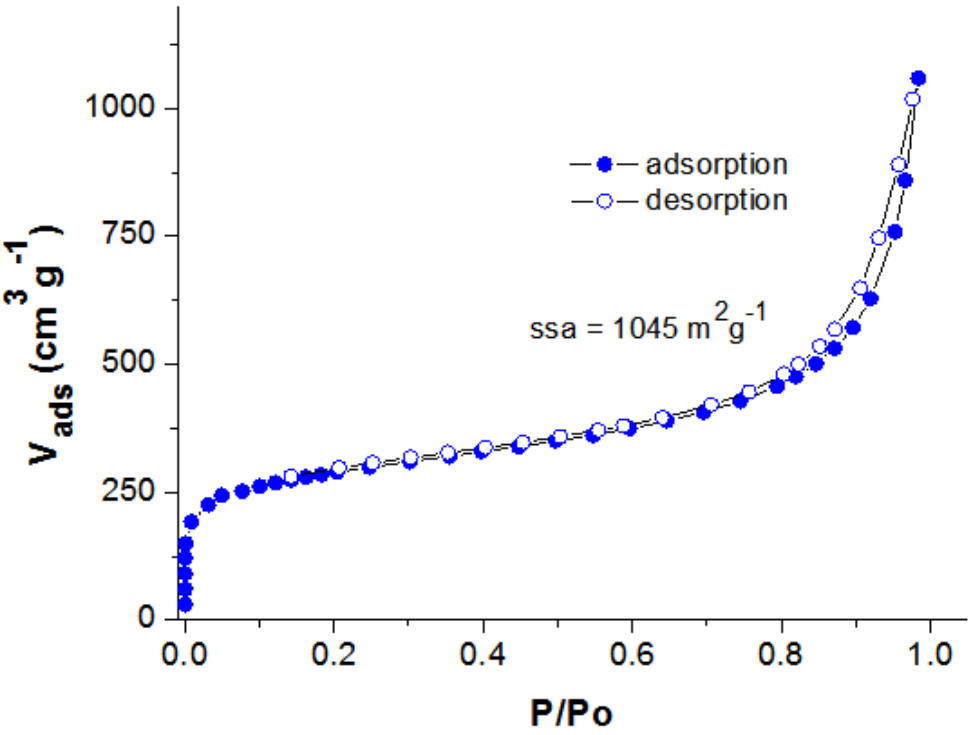

Figure S4. N_2 adsorption-desorption isotherm of uncapped POF **A1**-**B2** (Table S2, entry 1).

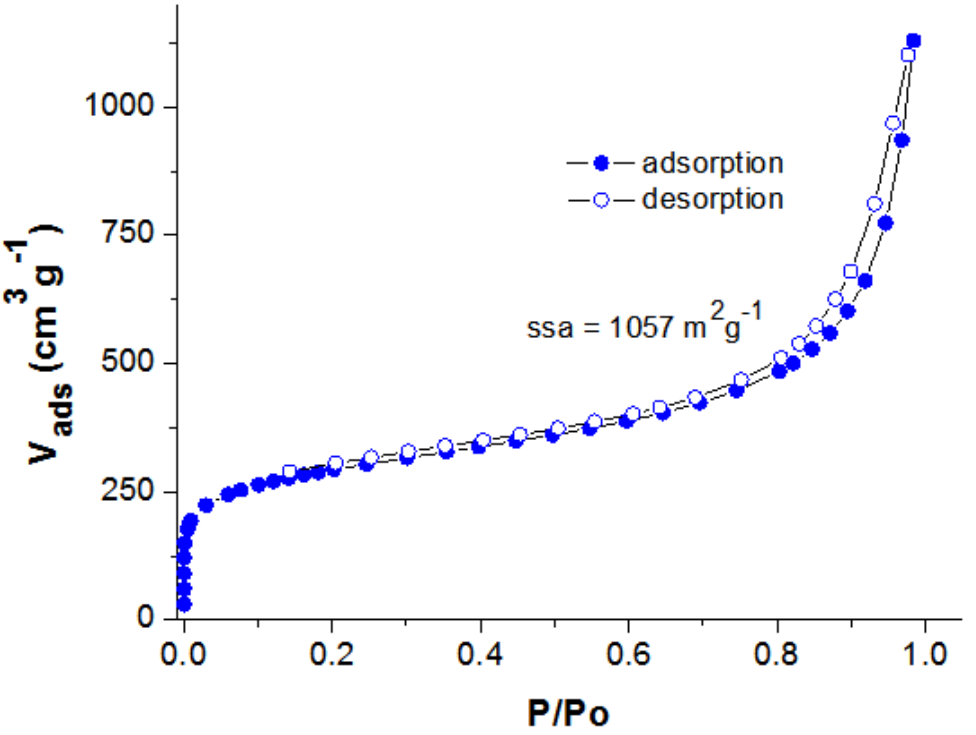

Figure S5. N_2 adsorption-desorption isotherm of aniline-capped POF **A1**-**B2** (Table S2, entry 2).

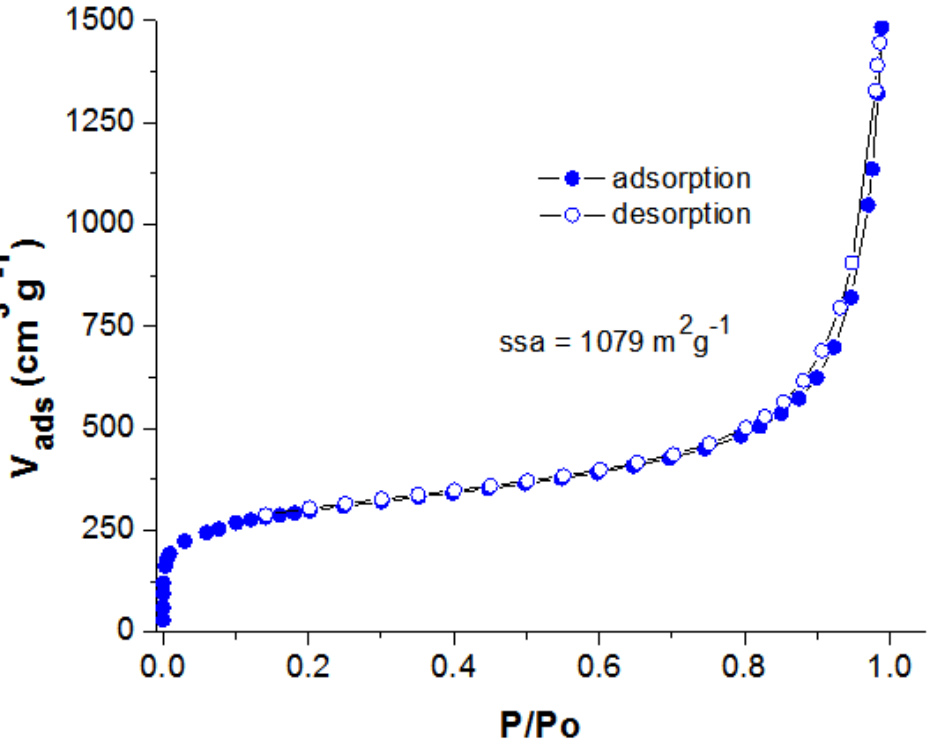

Figure S6. N_2 adsorption-desorption isotherm of benzaldehyde-capped POF **A1**-**B2** (Table S2, entry 3).

S4. N_2 adsorption-desorption isotherms of POFs.

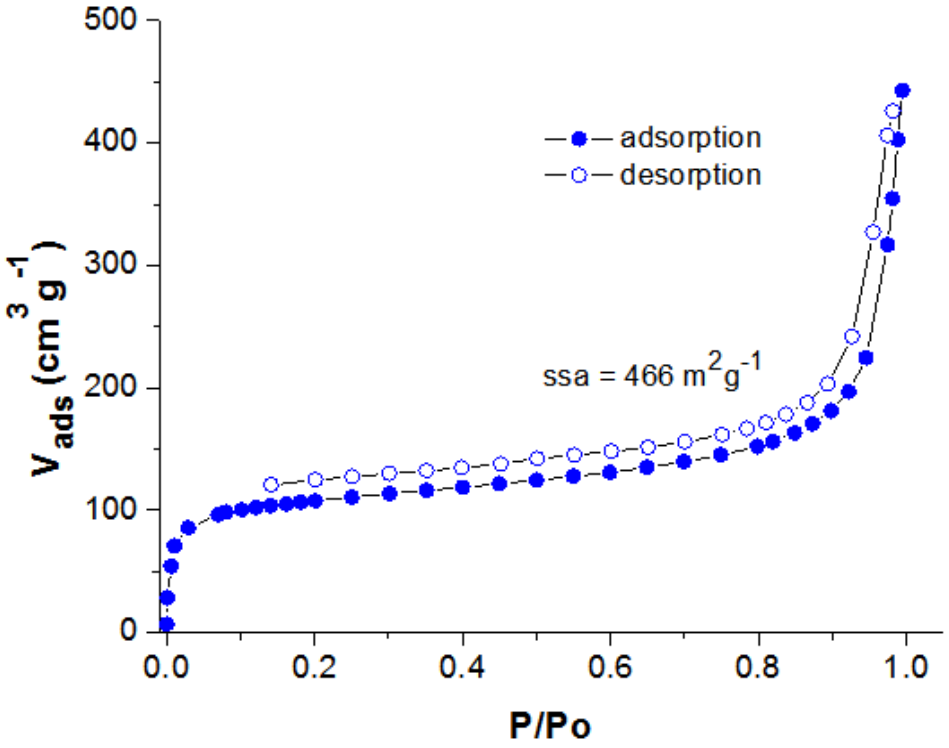

Figure S7. N_2 adsorption-desorption isotherm of POF **A1**-**B1** (Table 1, entry 1).

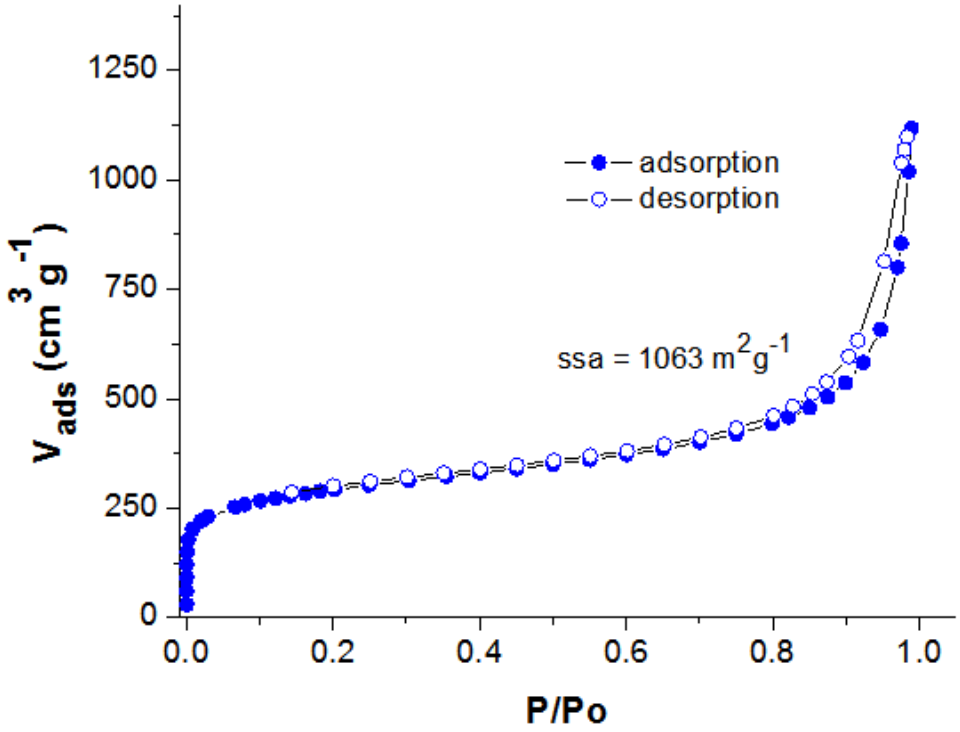

Figure S8. N_2 adsorption-desorption isotherm of POF **A1**-**B2** (Table 1, entry 2a).

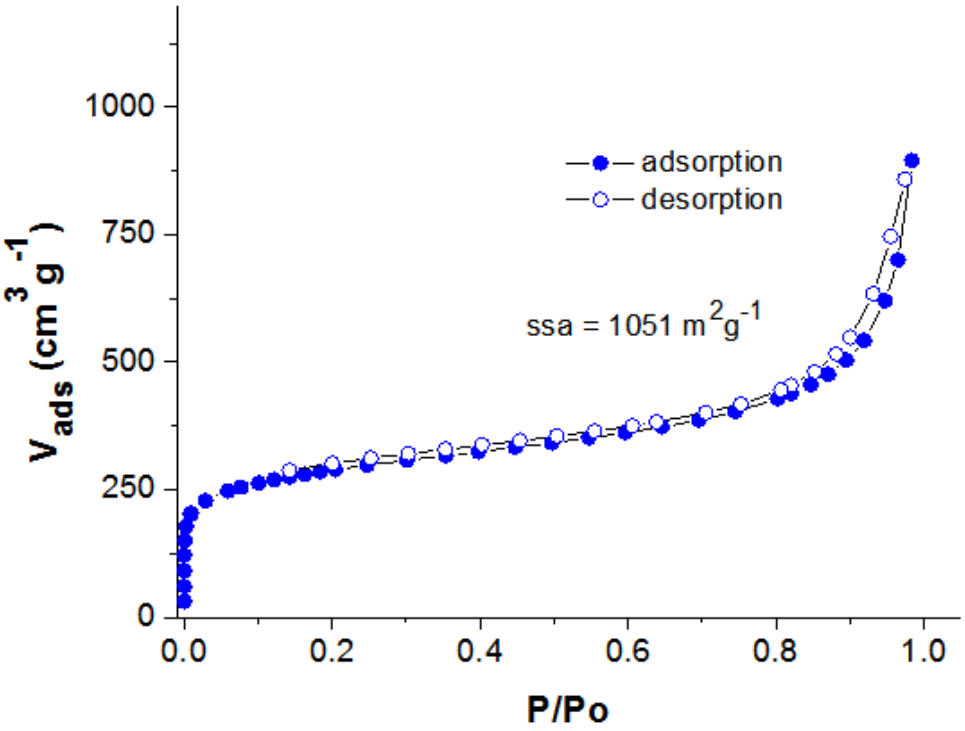

Figure S9. N_2 adsorption-desorption isotherm of POF **A1**-**B2** (Table 1, entry 2b).

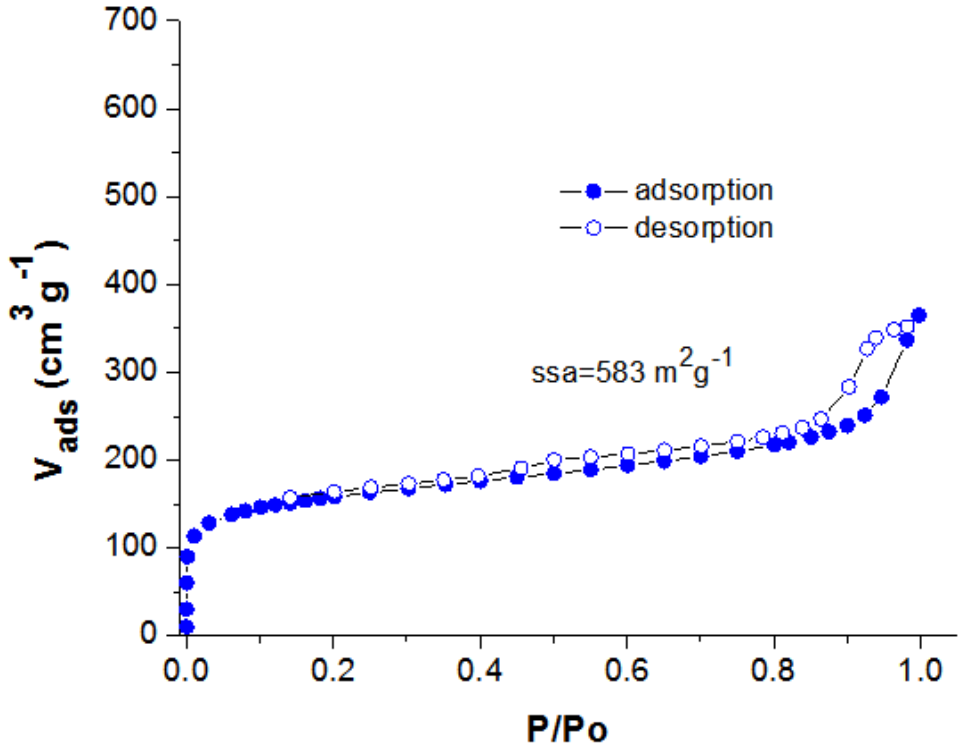

Figure S10. N_2 adsorption-desorption isotherm of POF **A1**-**B2** (Table 1, entry 2c).

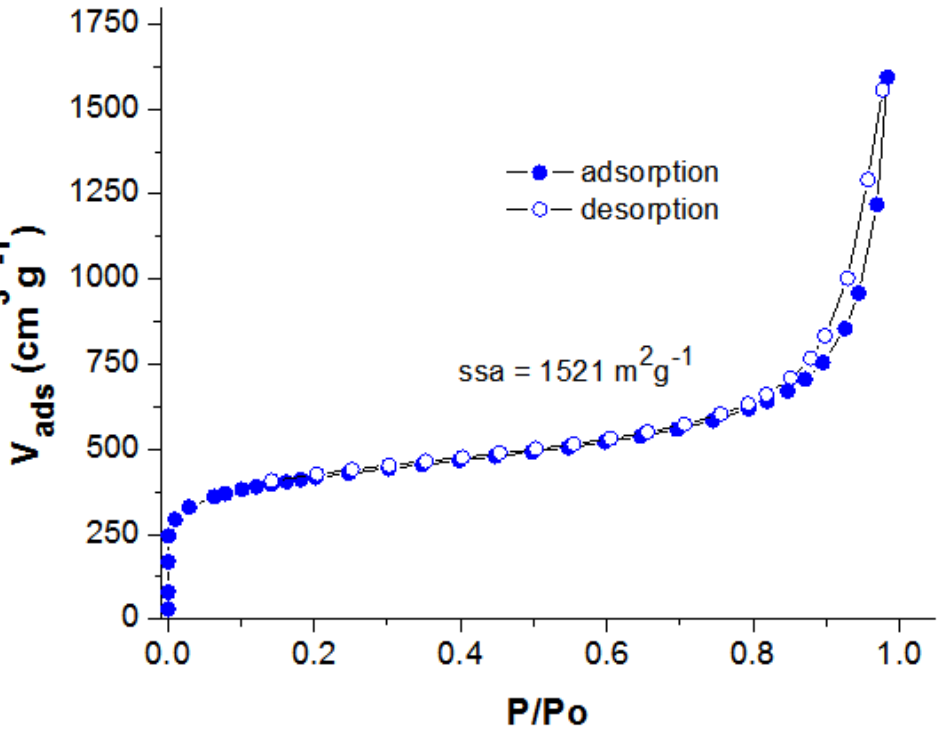

Figure S11. N_2 adsorption-desorption isotherm of POF **A1**-**B2** (Table 1, entry 2d).

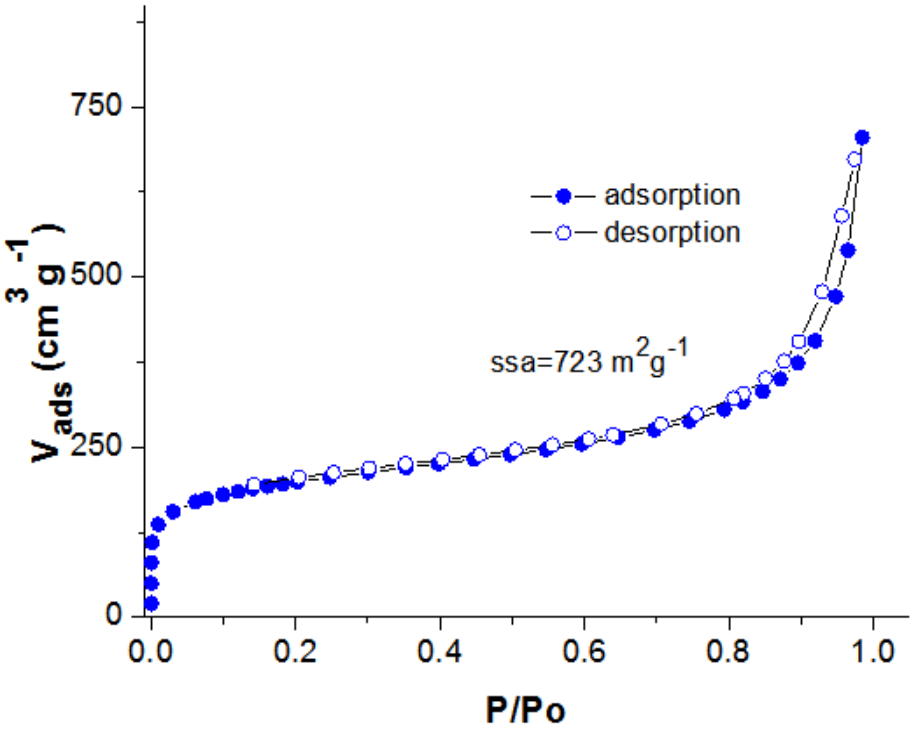

Figure S12. N_2 adsorption-desorption isotherm of POF **A1**-**B3** (Table 1, entry 3).

S5. FTIR spectra of monomers, model compound, and POFs.

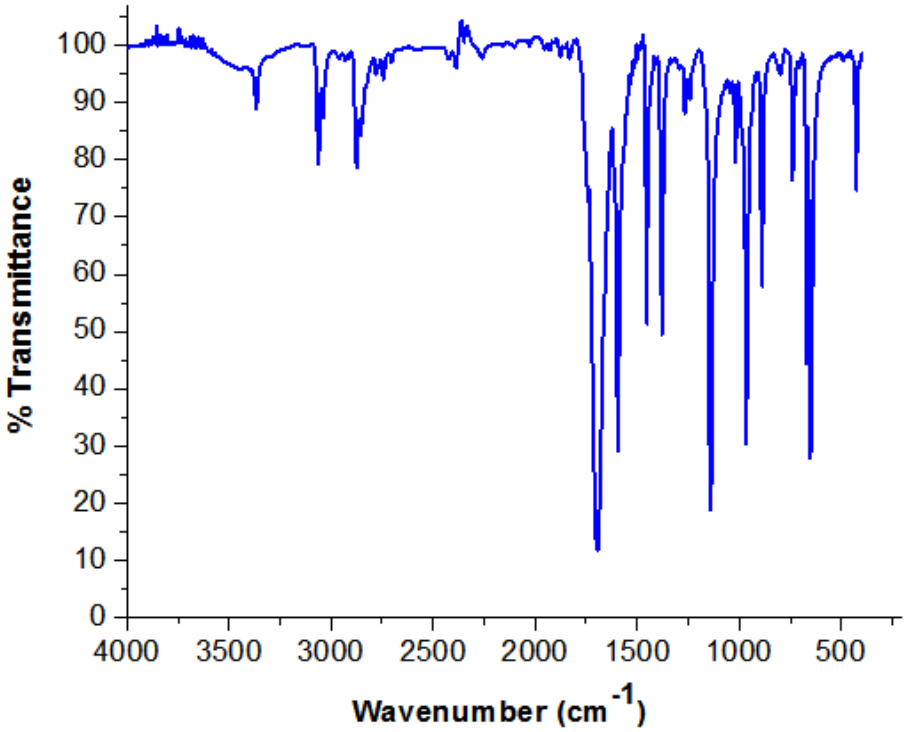

Figure S13. FTIR spectrum of 1,3,5-triformylbenzene (**A1**).

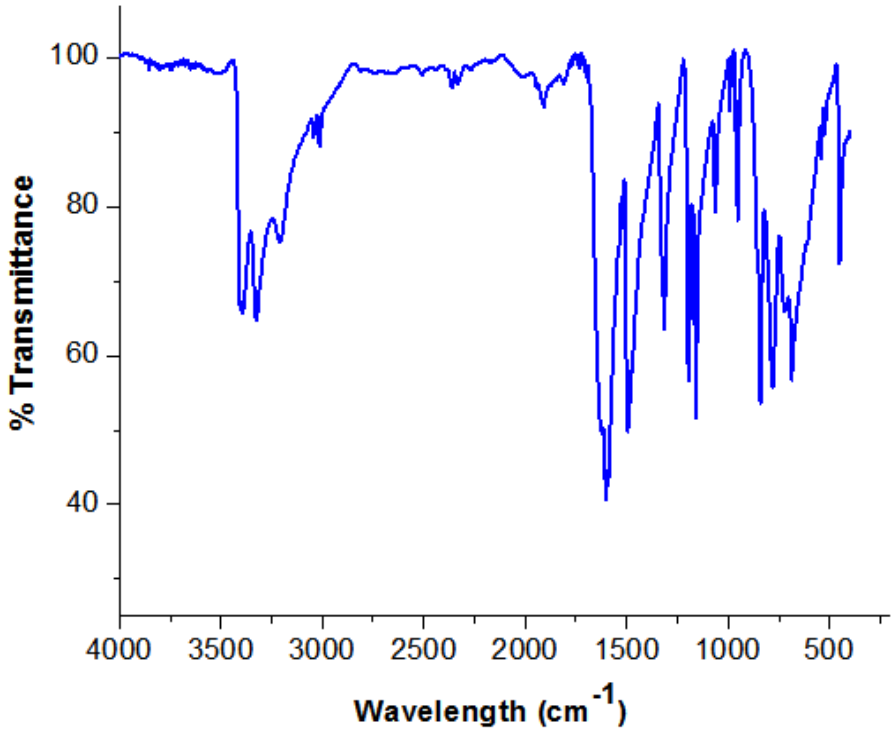

Figure S14. FTIR spectrum of 1,3-diaminobenzene (**B2**).

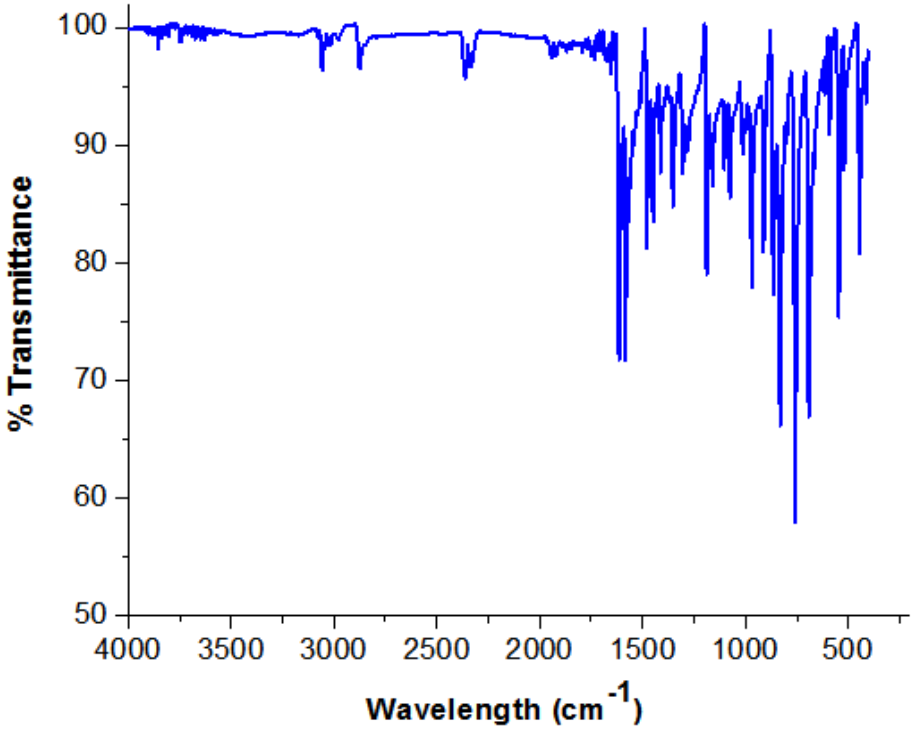

Figure S15. FTIR spectrum of the model compound (**MC1**).

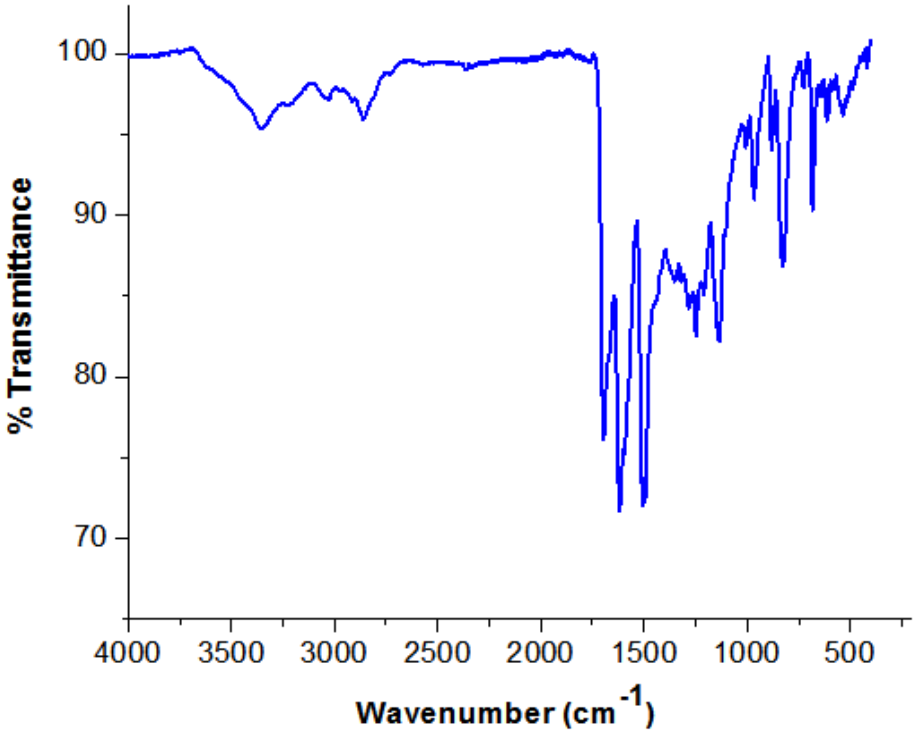

Figure S16. FTIR spectrum of POF **A1**-**B1** (Table 1, entry 1).

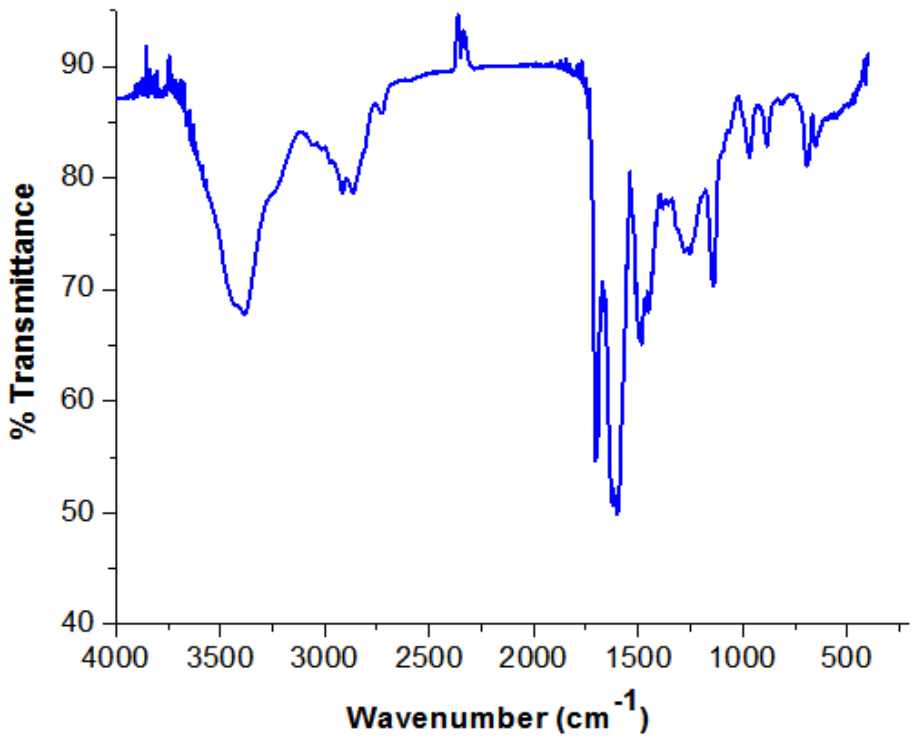

Figure S17. FTIR spectrum of POF **A1**-**B2** (Table 1, entry 2a).

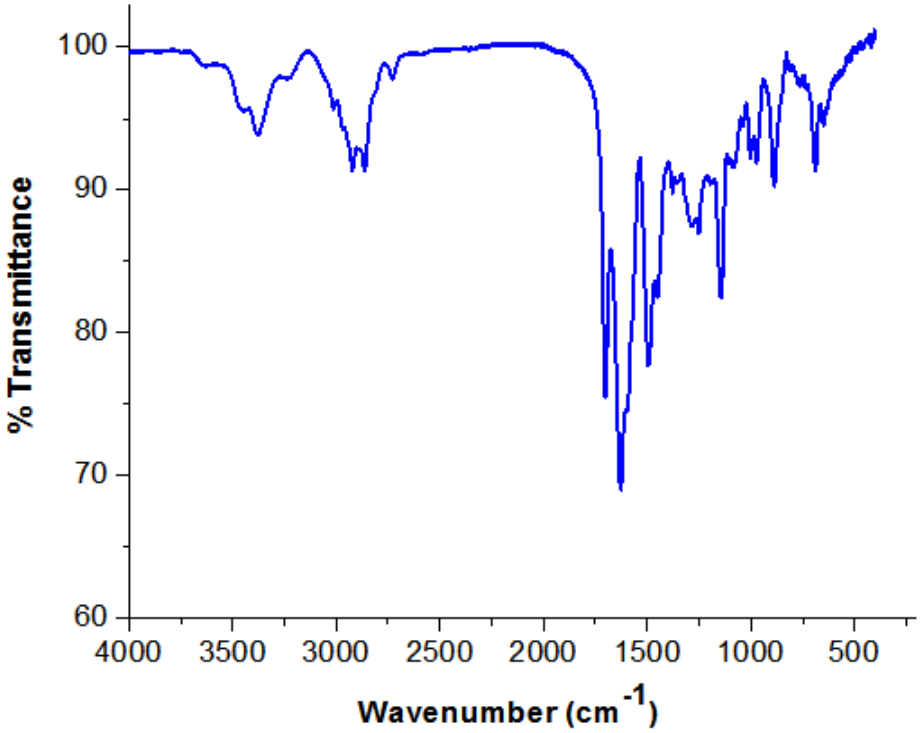

Figure S18. FTIR spectrum of POF **A1**-**B2** (Table 1, entry 2b).

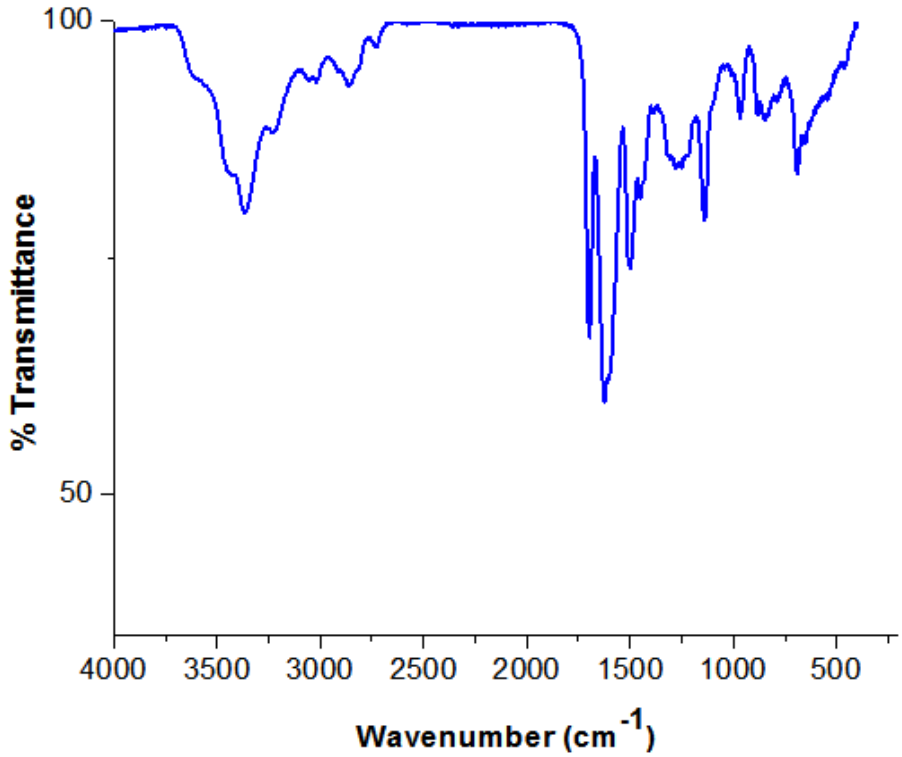

Figure S19. FTIR spectrum of POF **A1**-**B2** (Table 1, entry 2c).

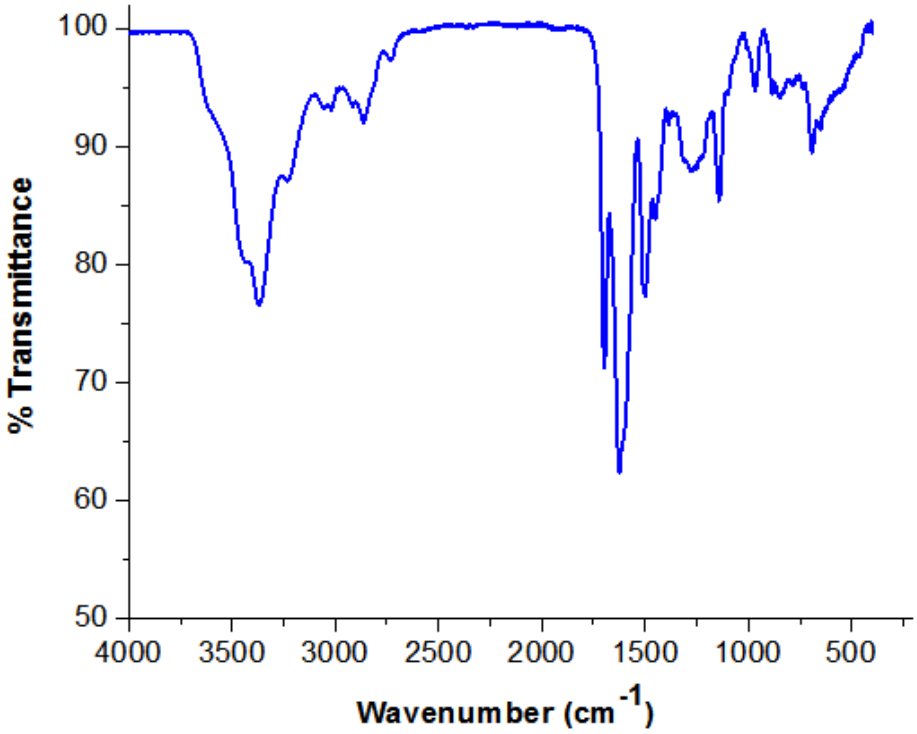

Figure S20. FTIR spectrum of POF **A1**-**B2** (Table 1, entry 2d).

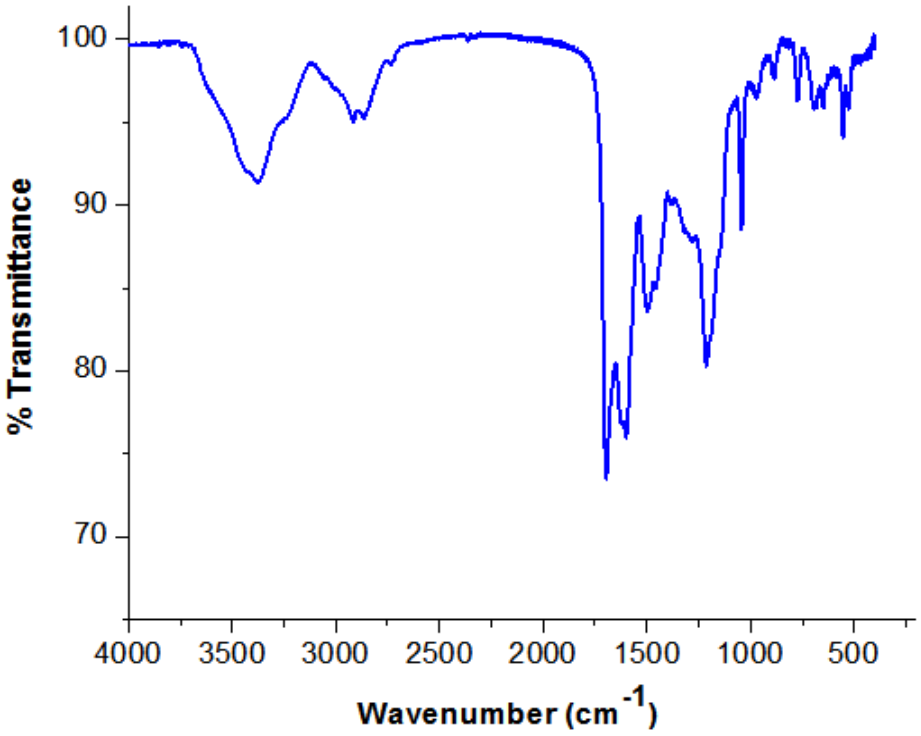

Figure S21. FTIR spectrum of POF **A1**-**B3** (Table 1, entry 3).

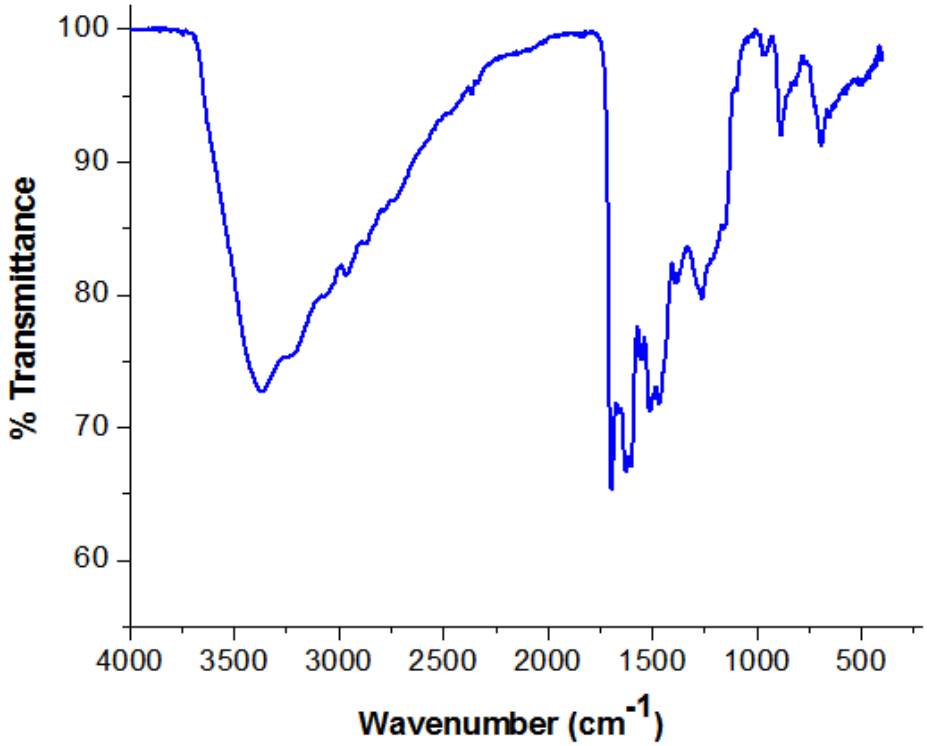

Figure S22. FTIR spectrum of POF **A1**-**B4** (Table 2, entry 3).

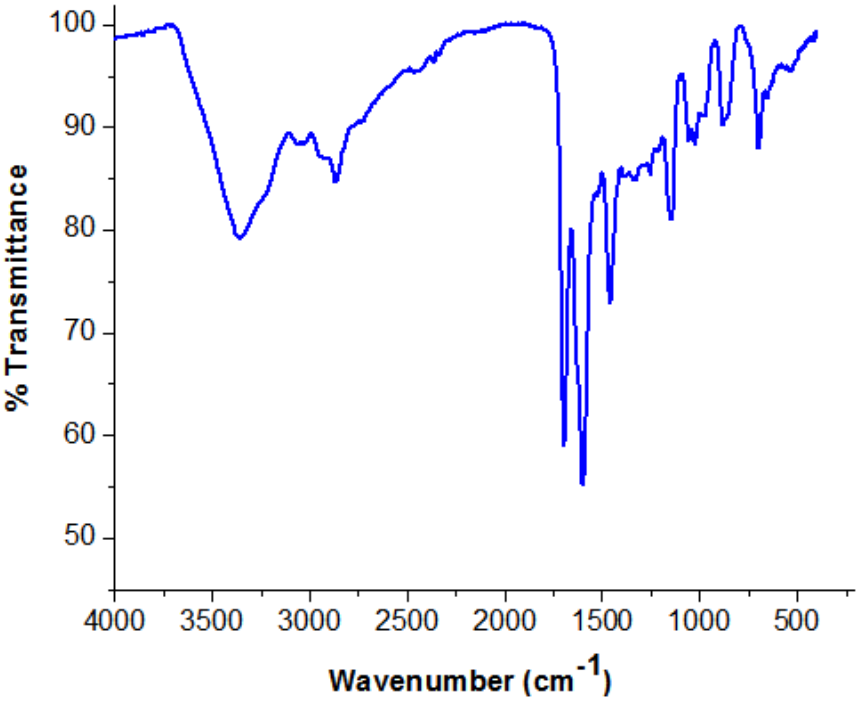

Figure S23. FTIR spectrum of POF **A1**-**B5** (Table 2, entry 4).

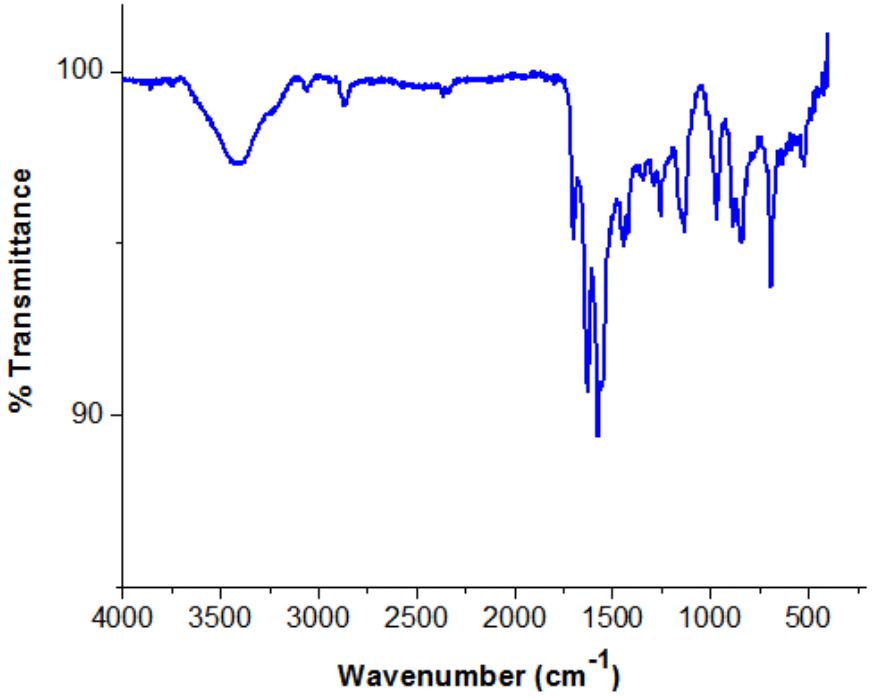

Figure S24. FTIR spectrum of POF **A1**-**B5** (Table 2, entry 5).

S6. H_2 and CO_2 adsorption isotherms of POFs.

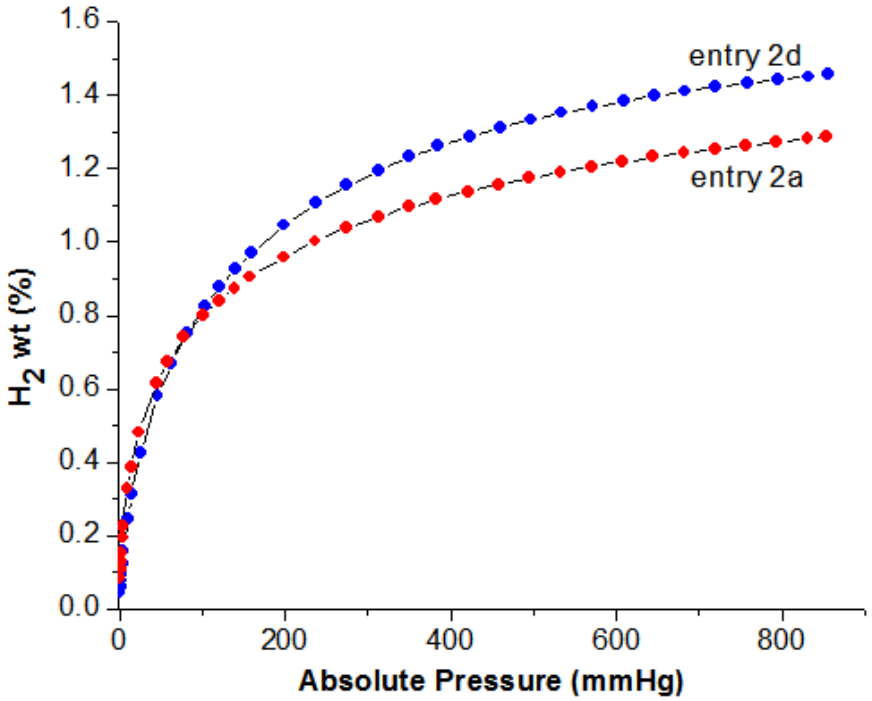

Figure S25. H_2 adsorption isotherms of POFs **A1-B2** (Table 1, entries 2a and 2d) at 77 K.

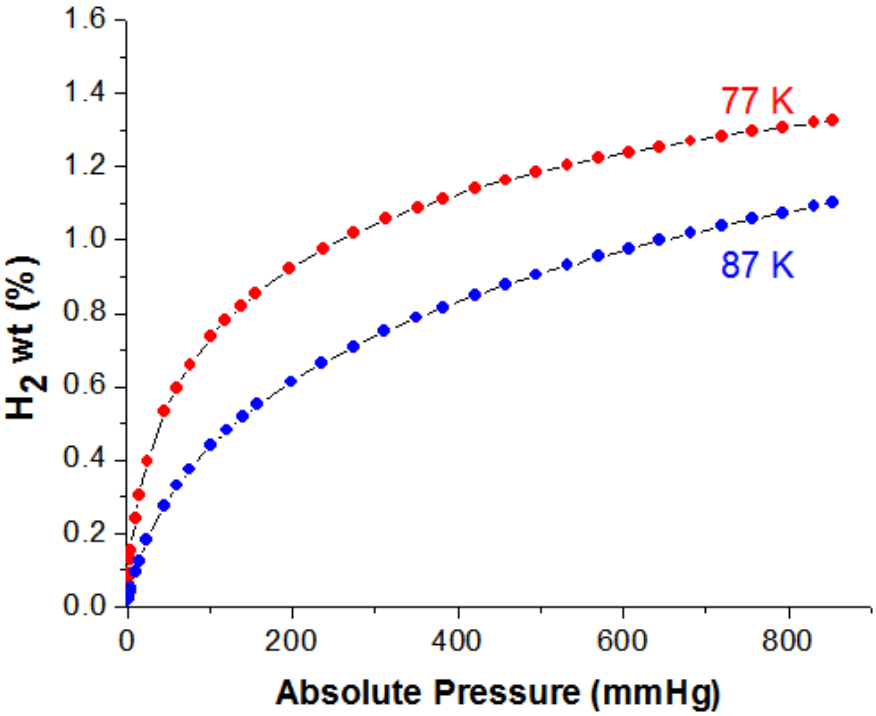

Figure S26. H_2 adsorption isotherms of POF **A1-B2** (Table 1, entry 2a) at 77 and 87 K.

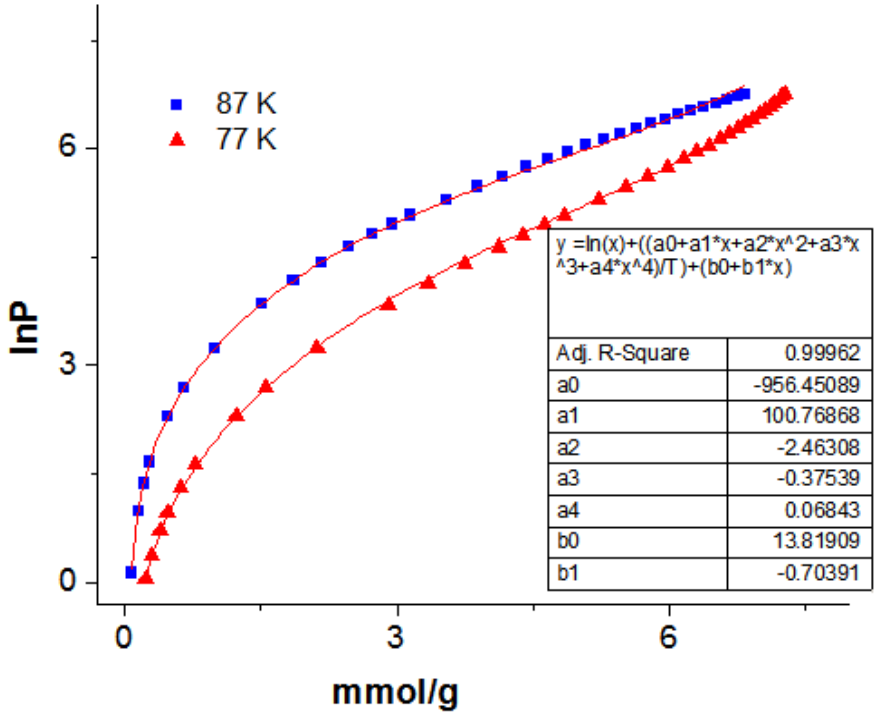

Figure S27. Fitting curves for H_2 adsorption isotherms of POF**A1**-**B2** (Table 1, entry 2a) at 77 and 87 K. Data are plot as the logarithm of pressure (mmHg) versus the adsorbed amount of gas (mmol g^{-1}).

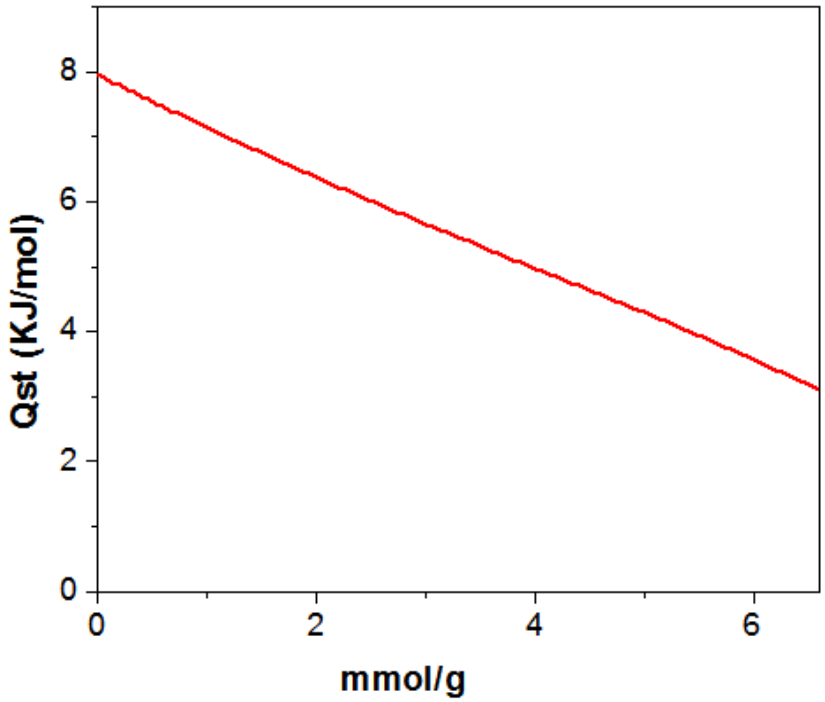

Figure S28. Isosteric heat of H_2 adsorption of POF **A1**-**B2** (Table 1, entry 2a).

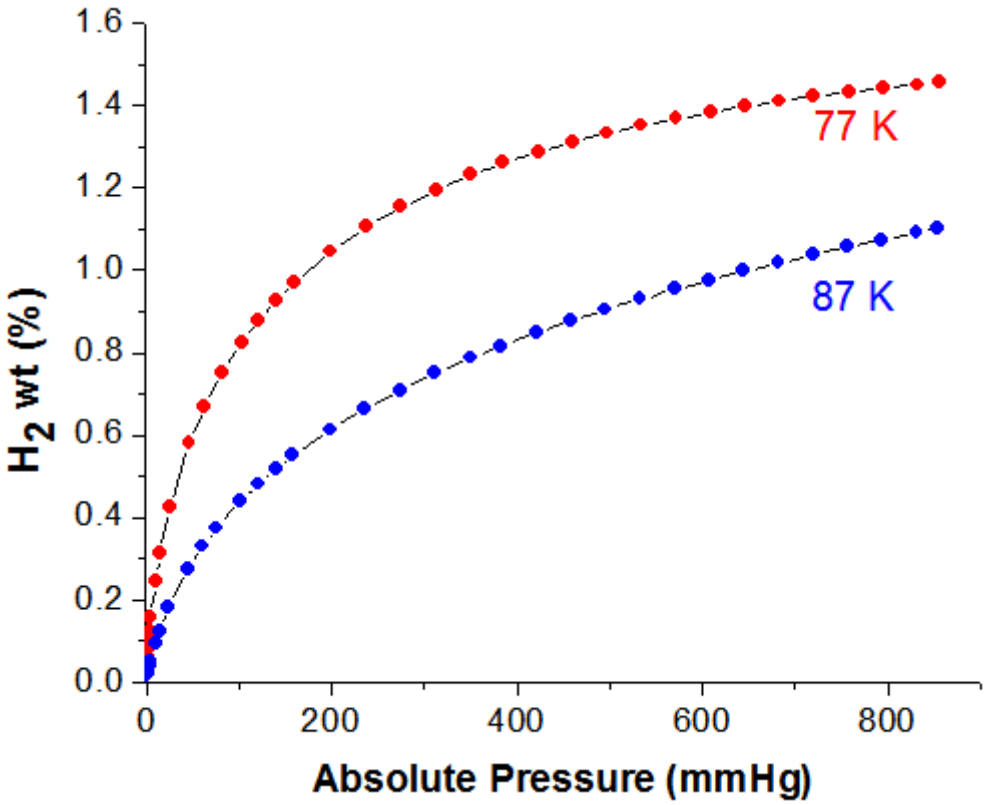

Figure S29. H_2 adsorption isotherms of POF **A1**-**B2** (Table 1, entry 2d) at 77 and 87 K.

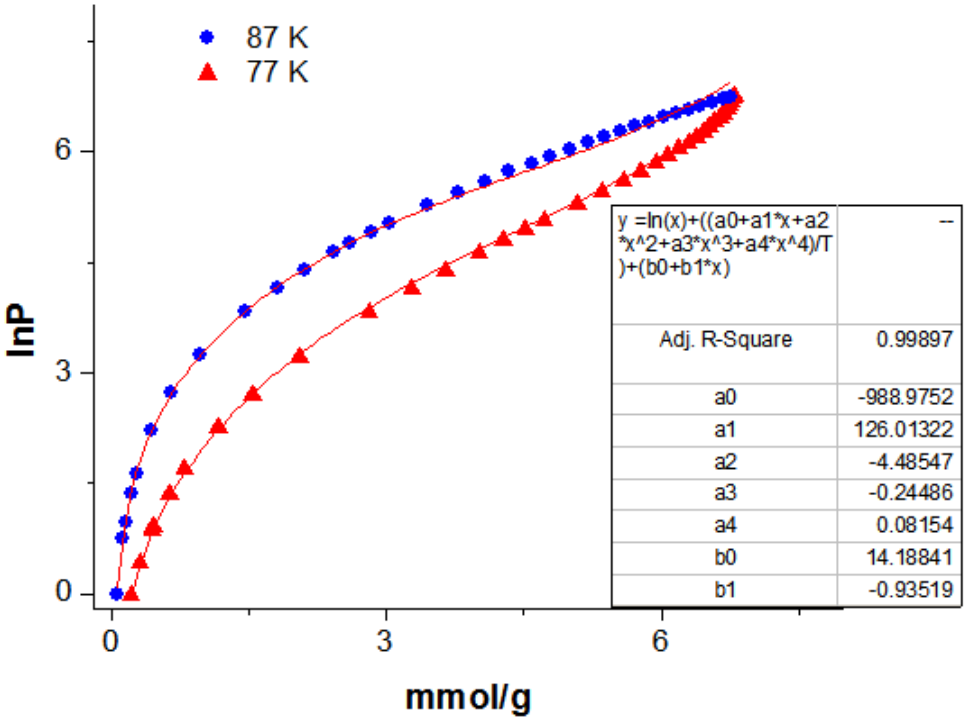

Figure S30. Fitting curves for H_2 adsorption isotherms of POF**A1**-**B2** (Table 1, entry 2d) at 77 and 87 K. Data are plot as the logarithm of pressure (mmHg) versus the adsorbed amount of gas (mmol g^{-1}).

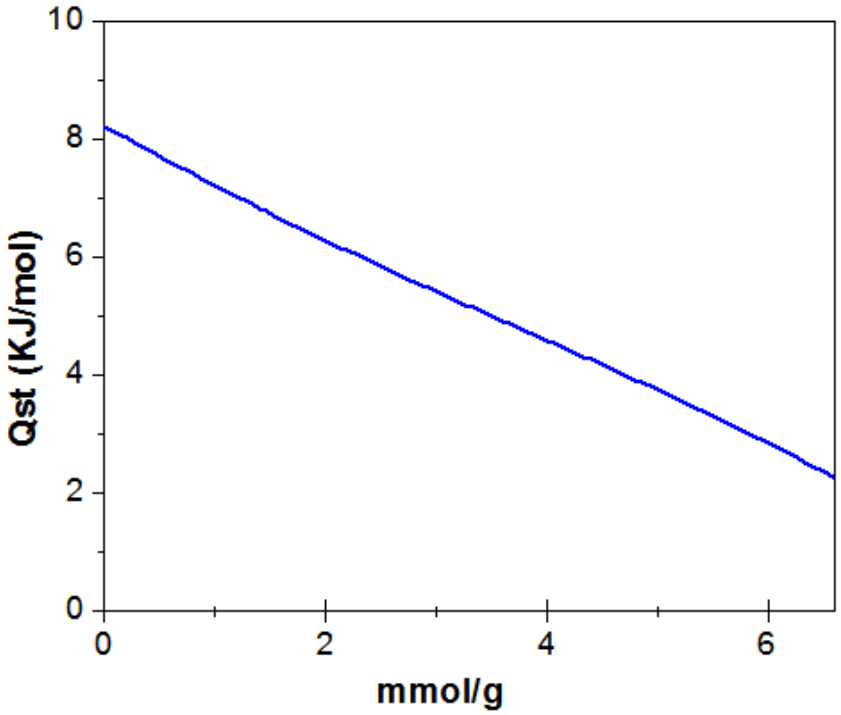

Figure S31. Isosteric heat of H_2 adsorption of POF **A1-B2** (Table 1, entry 2d).

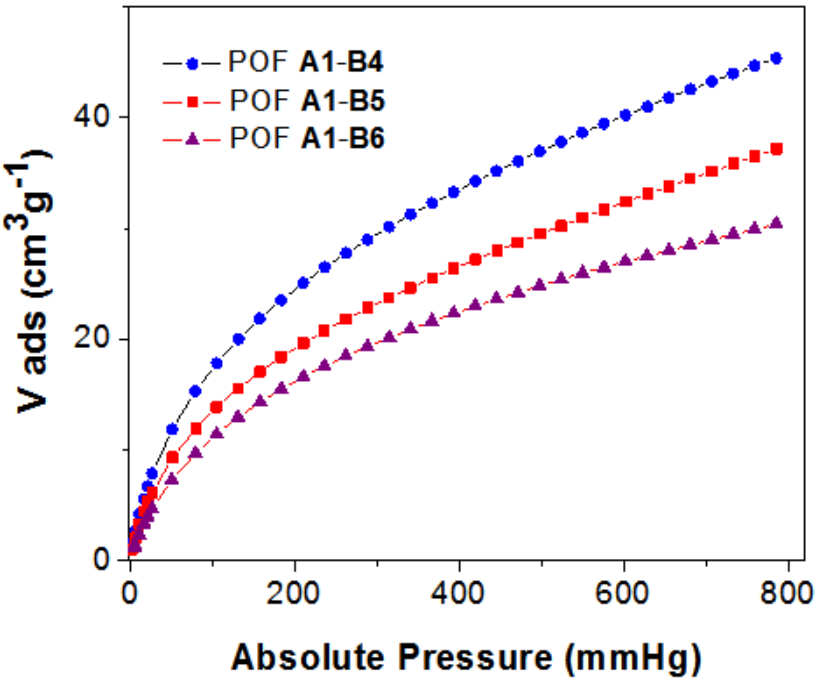

Figure S32. CO_2 adsorption isotherms of POFs **A1-B4** through **A1-B6** (Table 2, entries 3-5).

S7. Pore size distribution plots of POFs.

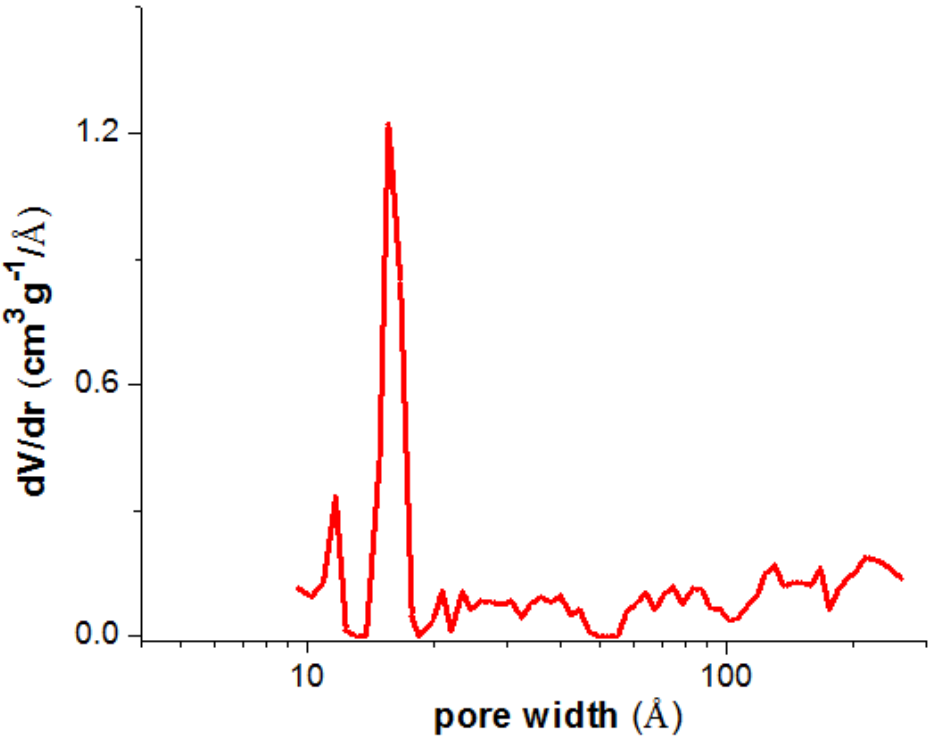

Figure S33. Pore size distribution of POF **A1**-**B1** (Table 1, entry 1) according to NLDFT.

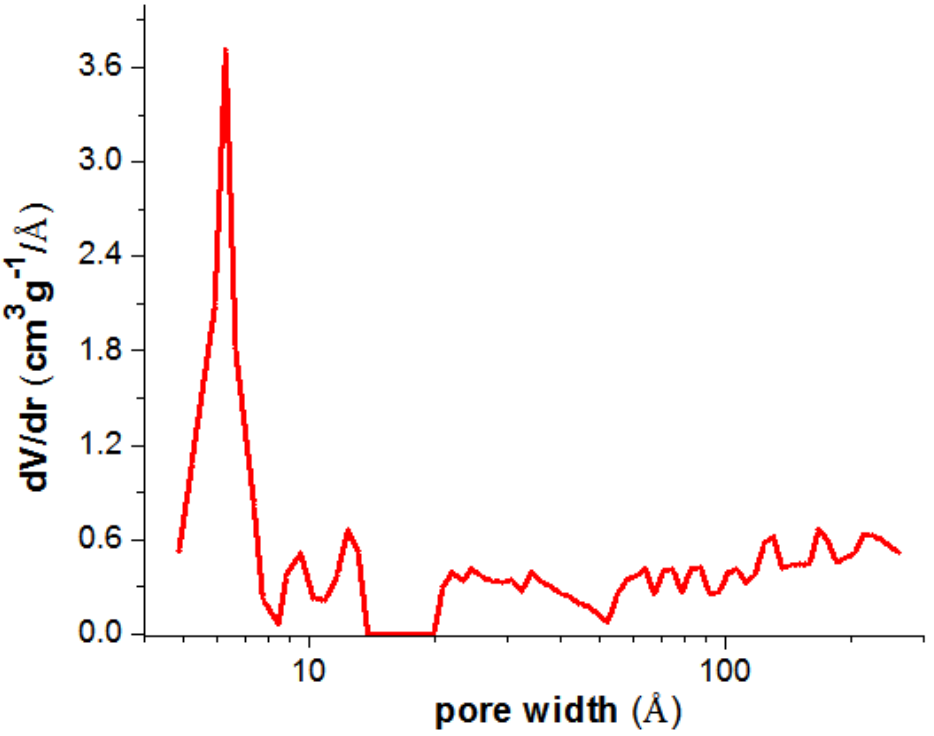

Figure S34. Pore size distribution of POF **A1**-**B2** (Table 1, entry 2a) according to NLDFT.

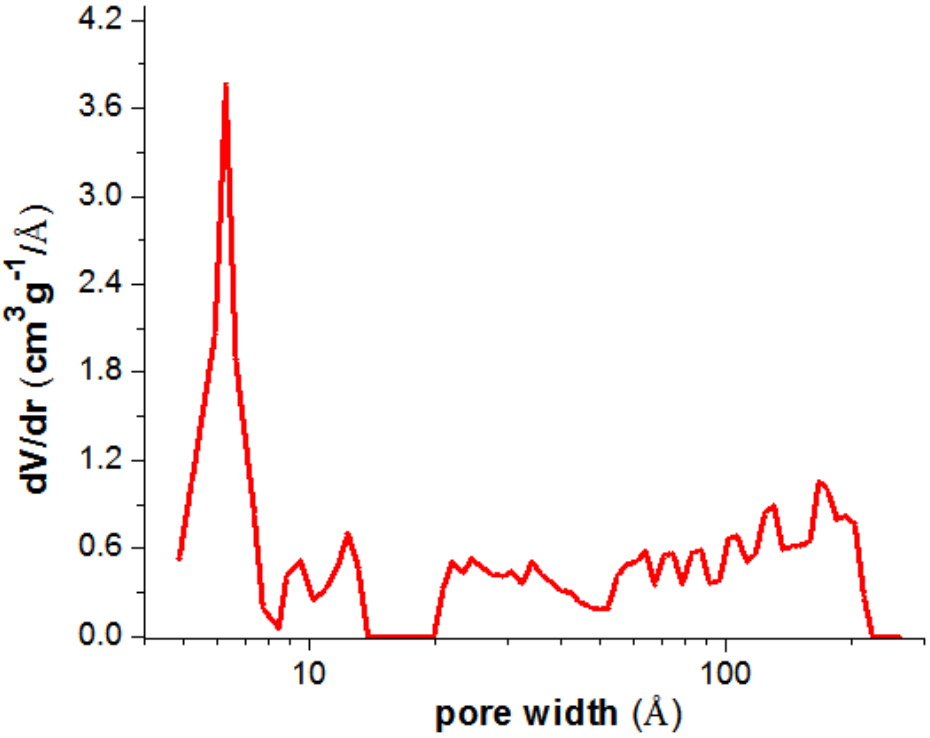

Figure S35. Pore size distribution of POF **A1**-**B2** (Table 1, entry 2d) according to NLDFT.

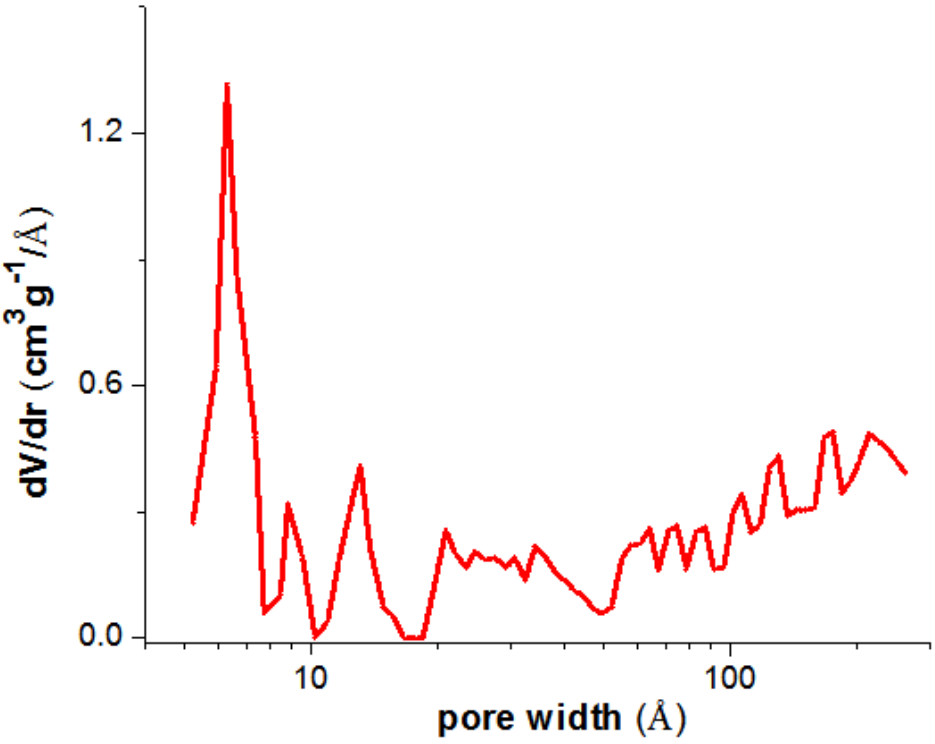

Figure S36. Pore size distribution of POF **A1**-**B2** (Table 1, entry 3) according to NLDFT.

S8. TGA profiles and SEM images of POFs.

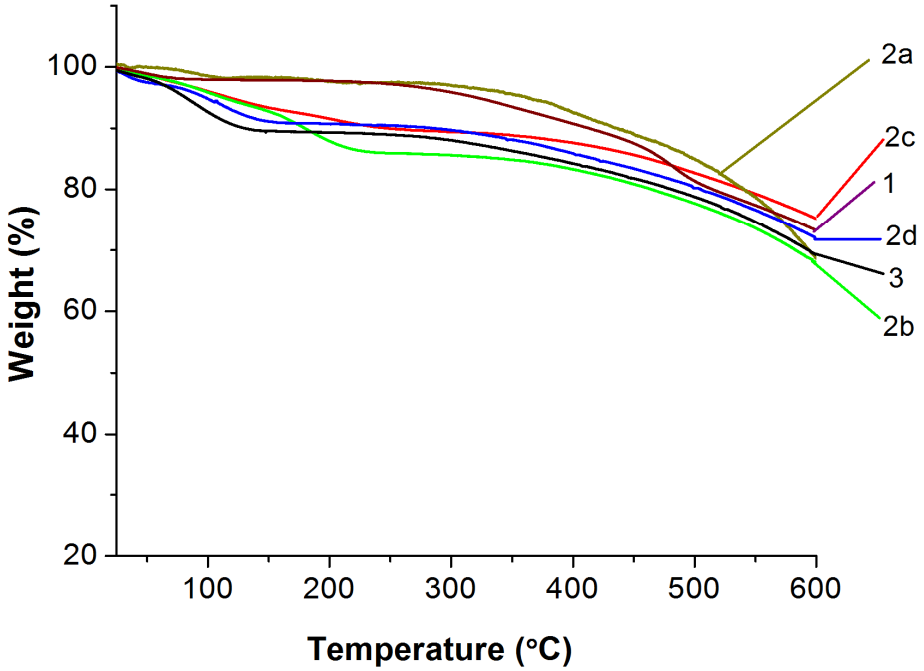

Figure S37a. Thermal gravimetric profiles of POFs **A1**-**B1** through **A1**-**B3** (Table 1, entries 1-3). The numbers on the peaks correspond to the entries in the table.

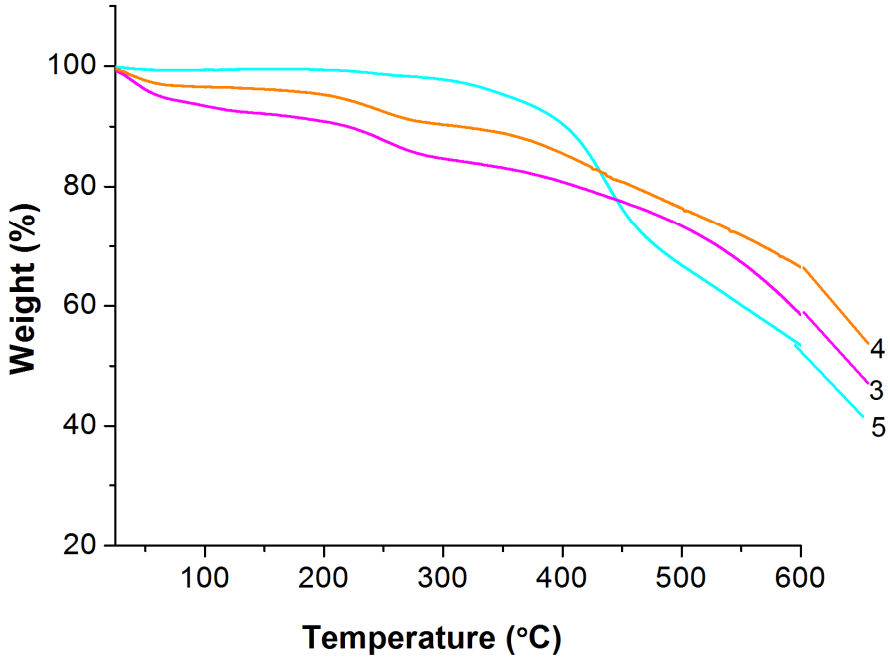

Figure S37b. Thermal gravimetric profiles of POFs **A1**-**B4** through **A1**-**B6** (Table 2, entries 3-5). The numbers on the peaks correspond to the entries in the table.

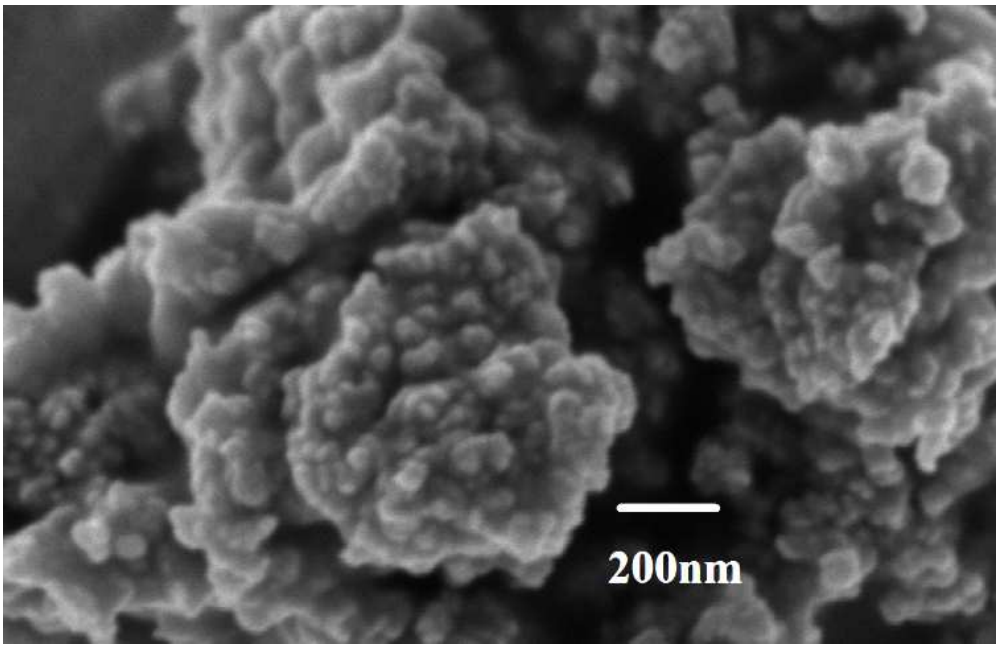

Figure S38. Scanning electron microscopy (SEM) image of POF **A1**-**B1** (Table 1, entry 1)

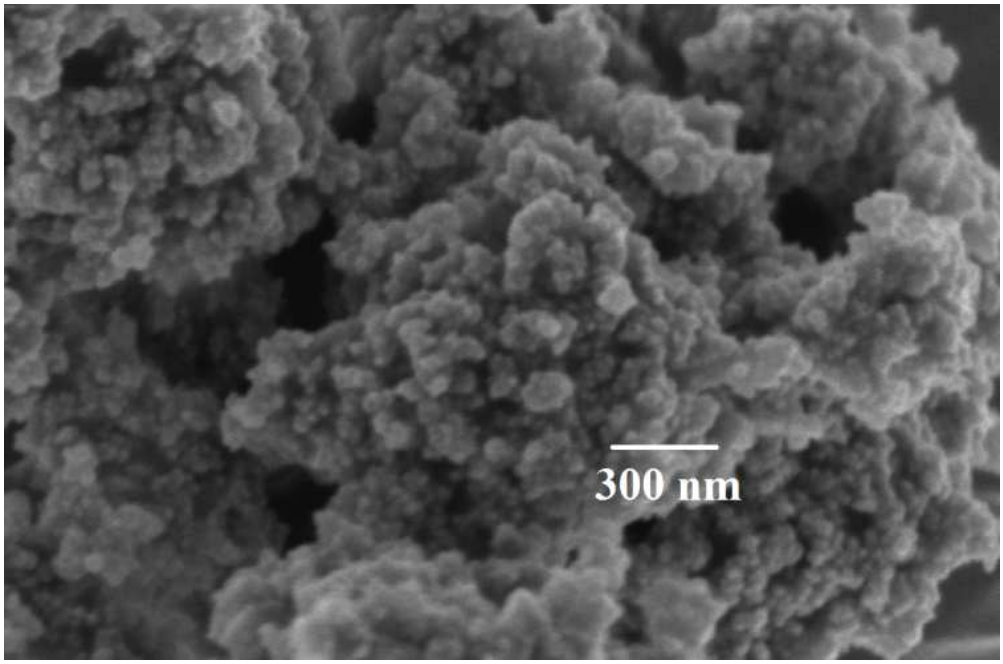

Figure S39. Scanning electron microscopy (SEM) image of POF **A1**-**B2** (Table 1, entry 2a). POFs **A1**-**B2** through **A1**-**B6** show similar aggregated nanoparticle morphology.

S9. Stability of POF A1-B2.

While our as-synthesized materials are stable over several months in ambient conditions (i.e., no apparent loss of masses or morphology), their surface areas decrease by about 20% within a week and then stabilize over the next several months after 30% decrease in surface area (Table S8 in SI). This initial loss of surface areas is attributed to framework relaxation and not due to prolonged exposure to ambient moisture: the loss in surface area occurs when we stored the materials (for example, POFs **A1**-**B2**) in either a capped-vial or open to ambient atmosphere on a bench top, it occurs even when we kept the as synthesized in a sealed tube under vacuum or in a dessicator (Table S8).

When POF **A1**-**B2** is stirred in water for 12 h, there is minimum mass loss; however, its surface area is reduced by ~25%. After 24 h in water, its surface area decreases by about 40%.

Table S8. Surface area analysis of POF **A1-B2** tested under different conditions.

Entry	POF **A1**-**B2**	Specific surface area ($m^2 g^{-1}$)	Micropore volume ($cm^3 g^{-1}$)	Total pore volume ($cm^3 g^{-1}$)
1	as-synthesized (entry 2a, Table 1)	1063	0.31	1.13
2	left in an open vial for 5 days	843	0.29	0.79
3	left in an open vial for 30 days	723	0.26	0.77
4	left in a capped vial for 30 days	760	0.29	0.80
5	left in a dessicator containing Drierite for 30 days	745	0.27	0.83
6	left in a sealed tube under vacuum for 30 days	764	0.30	0.85
7	left in a capped vial for 90 days	734	0.26	0.83
8	stirred in water for 12 h	751	0.25	0.85
9	stirred in water for 24 h	603	0.21	0.62

References

(S1) Dimick, S. M.; Powell, S. C.; McMahon, S. A.; Moothoo, D. N.; Naismith, J. H.; Toone, E. J. *J. Am. Chem. Soc.* **1999**, *121*, 10286-10296.

(S2) Kaur, N.; Delcros, J.-G.; Imran, J.; Khaled, A.; Chehtane, M.; Tschammer, N.; Martin, B.; Phanstiel, O. *J. Med. Chem.* **2008**, *51*, 1393-1401.

(S3) Schwab, M. G.; Fassbender, B.; Spiess, H. W.; Thomas, A.; Feng, X.; Müllen, K. *J. Am. Chem. Soc.* **2009**, *131*, 7216-7217.

(S4) Suggs, J. W. *J. Am. Chem. Soc.* **1979**, *101*, 489-489.

(S5) Tiollais, R.; Bouget, G.; Bouget, H. *C. R. Hebd. Seances Acad. Sci.* **1962**, *254*, 2597-2600.

(S6) Duhamel, L. In *The Chemistry of amino, nitroso and nitro compounds and their derivatives*; Patai, S., Ed.; John Wiley & Sons Ltd.: Binghamton, N.Y., 1982, p 849-907.

(S7) Eibner, A. *Chem. Ber.* **1897**, *30*, 1444-1450.

(S8) Miller, J. G.; Wagner, E. C. *J. Am. Chem. Soc.* **1932**, *54*, 3698-3706.